TARGETING POD EFFECTS ON WEAPONS RELEASE FROM THE F-18C HORNET

William H. Godiksen III*, Eric N. Hallberg*
***US Naval Academy**

Keywords: *store separation, computational fluid dynamics, CFD, TFLIR, ATFLIR, F-18*

Abstract

In December of 1998 during routine bombing practice at Fallon, NV, an F-18C released a Mark 82 JDAM bomb which impacted the Targeting Forward-Looking Infrared Pod (TFLIR) on the aircraft fuselage. This study investigated the efficacy of CFD to predict and explain the effects the TFLIR, the ATFLIR, and the Litening pod on the store separation characteristics of the F-18C. It was found that the tapered trailing surface of the ATFLIR pod caused a strong shockwave to form approaching Mach 1.0, and it was this shockwave crossing the tail fins of the weapon that caused the adverse change in trajectory. CFD analysis revealed that the TFLIR and Litening pods caused weaker shocks off their aft ends. Furthermore, the extended length of the Litening pod caused the aft shock to impinge less on the adjacent store tail fins. Trajectory simulation predictions were accomplished using the Navy Generalized Separation Package (NAVSEP) and results from these predictions compared favorably with flight test results. Design changes to the aft geometry of the pods are proposed which have the potential to create a safer and more combat-effective fighter.

1 Introduction

In order to establish safe flight conditions for the release of bombs or other stores from attack aircraft, the Navy conducts flight tests at various aircraft attitudes, Mach numbers, and store configurations and determines the initial path taken by the falling store. This determination of path is generally made using a series of high speed photographs, known as photogrammetrics, or the analysis of data taken from an accelerometer located on the store itself, known as telemetry. Though very accurate, many such flight tests are necessary in order to approve a range of acceptable flight conditions, and these are costly in both time and money. In the absence of pre-flight analysis, the most benign flight condition is chosen as the starting point of the flight test, typically fully sub-sonic. The release envelope is gradually expanded through subsequent releases by increasing the Mach number and altitude. Many such flights are required to reach the boundary of the aircraft flight envelope.

The number and duration of flights required can be significantly reduced by predicting trajectories before flights are begun. This pre-flight flow analysis is accomplished in both the wind tunnel and through computational fluid dynamics (CFD). Prior to any flight testing, predicted trajectories are obtained using one or both of these methods, and these results are used to determine which configurations require flight tests and to what extent. For instance, a clearance to Mach 0.97 may require a build-up approach beginning at a benign flight condition such as Mach 0.88 and progressing up to Mach 0.97 at steps of 0.02 Mach. Extensive wind tunnel and CFD analysis could permit fewer steps in the build-up to the endpoint if CFD and wind tunnel analysis shows the endpoint to be safe, and interim flight test steps match predictions.

1.1 Background

The inspiration for this research began with routine bombing practice conducted in Fallon,

Nevada in December of 1998. The pilot was flying an F-18C aircraft with a Targeting Forward-Looking Infrared Pod (TFLIR) mounted on the side of the plane's fuselage and a Mark-82 bomb hanging from the inboard wing pylon adjacent to the targeting pod. Figure 1 below shows an F-18C aircraft with a TFLIR attached and a fuel tank on the inboard pylon.

Fig 1. TFLIR pod mounted on F-18C

When the pilot dropped the Mark 82 from his aircraft, the nose of the bomb yawed away from the fuselage and caused the bomb's tail fins to impact the TFLIR. This result was unexpected as this flight condition had been cleared for safe release in the aircraft's tactical manual. An investigation soon revealed that the TFLIR was considered a part of the aircraft and that its effect on store separation had been assumed to be negligible. As a result, neither wind tunnel nor flight testing had been done to determine what effect it might have. After this incident, the Navy decided to begin a flight test program in order to establish safe release parameters. [1]

At this same time the Navy introduced the Advanced Targeting Forward Looking Infrared Pod (ATFLIR), which is geometrically similar to the TFLIR but significantly more capable. A picture of the ATFLIR pod mounted on an F-18C can be seen below in Figure 2. The main difference in shape between these two pods is the fairing on the leading edge of the ATFLIR, which is not present on the TFLIR. In most other aspects, these pods look essentially identical. There are subtle differences in the geometry of the trailing end of the pods which were initially not thought to be significant compared to the larger differences in their front-end geometries. This research showed this assumption to be wrong.

Fig 2. ATFLIR pod mounted on F-18C [2]

This pod was examined in the flight test program in the same manner as the TFLIR. It was expected that the ATFLIR would have nearly the same effect on the aircraft's flowfield as the TFLIR due to their geometric similarity. However, flight test results soon proved otherwise. At speeds just under the speed of sound, between Mach 0.90 and 0.95, the flight test results showed significant differences in the trajectories of bombs dropped next to the TFLIR versus those beside the ATFLIR. Although the cause of this variance was not understood, time and schedule constraints precluded further research. The flight test program concluded by restricting the release of certain stores in proximity to either targeting pod to a subset of the full combat aircraft flight envelope.

While these test flights were successful in establishing safe store release conditions for these pods, they did not produce a full understanding of the effect of the (A)TFLIR pod on the F-18C flowfield. Furthermore, the full operating envelope of the combat aircraft was restricted. Analysis of this release condition is challenging. The geometric differences between the two pods are subtle and the flowfield at the Mach number of interest is fully transonic with a number of shocks forming and moving as the store is released. Computational Fluid Dynamics is an ideal choice for analysis of this scenario.

2 Computational Analysis

A systematic approach has been used throughout this research project in order to produce accurate and replicable data. The first phase consisted of validation of the F-18C model using previously generated wind tunnel data. The validation metric was a comparison of the flow properties in the vicinity of the store carriage location. The TFLIR and ATFLIR were then added to this model and their effects on the flowfield were analyzed. The model of the GBU-31 JDAM was obtained and validated next, again using existing wind tunnel data. The validation metric was the normal force and pitching moment on the store. After validation, the JDAM was attached to the F-18C both with and without the targeting pods attached, and the various solution results were analyzed.

2.1 F-18C Model Validation

The first step in the research process consisted of manipulating the geometry of the aircraft to be used, the F-18C Hornet. This aircraft was chosen because it was involved in the initial mishap and is one of the principle platforms that uses the TFLIR and ATFLIR pods. Fortunately, the geometry of this aircraft had already been used with GridTool, so very little work was needed to prepare the model for grid generation. Using VGRID and USM3D, solutions were soon generated for the clean (no pods or stores) configuration at Mach numbers of 0.8 and 0.95. These speeds were chosen to allow comparison with wind tunnel data previously obtained at these Mach numbers. The particular wind tunnel data used were generated in tests at the David Taylor Research Center transonic wind tunnel in 1989-1990.

The measurements taken at this point were recordings of the upwash and sidewash angles at various points in the flow. Because the axial component is much larger than both the normal and vertical velocity components, these angles will rarely exceed 5º in magnitude. In the wind tunnel experiment these angles were measured along an axial flow line beneath the inboard pylon. Figure 3 below shows where this line was located in reference to the aircraft, with the flow line colored red. This same flow line was analyzed in this project using CFD in order to facilitate comparison.

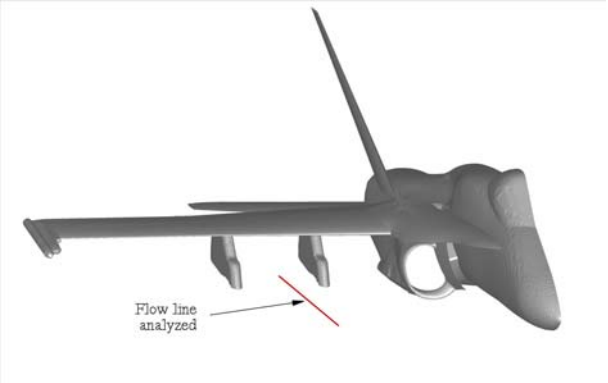

Fig 3. Axial flow line beneath pylon

Analysis of the CFD solutions was accomplished using the post-processing software Tecplot®, which enabled extraction of the flow velocity components along the same flow line tested in the wind tunnel. The CFD results were then plotted against the wind tunnel results, and the resulting plots can be seen below in Figures 4-7, which are at Mach 0.8 and 0.95.

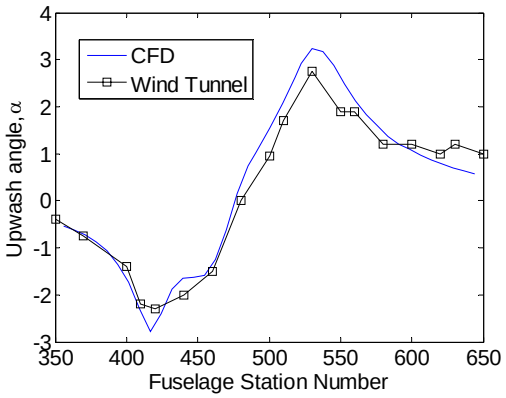

Fig 4. Upwash angle comparison at Mach 0.8

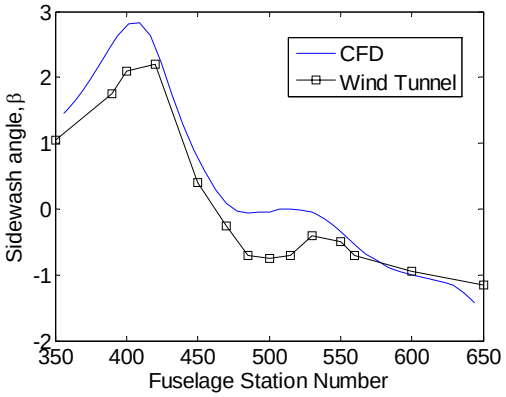

Fig 5. Sidewash angle comparison at Mach 0.8

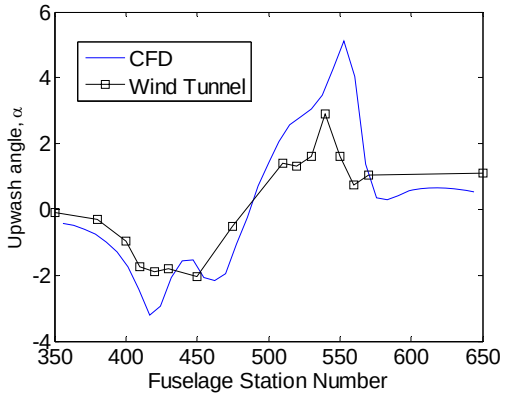

Fig 6. Upwash angle comparison at Mach 0.95

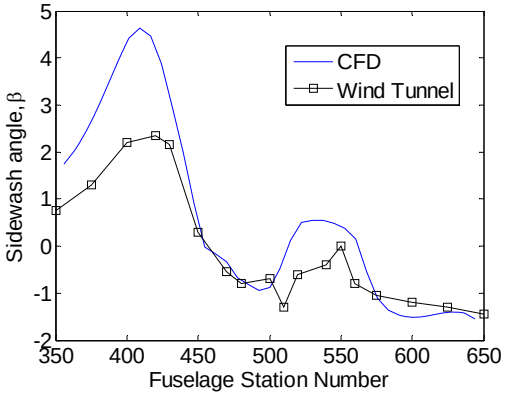

Fig 7. Sidewash angle comparison at Mach 0.95

The horizontal axis of these figures is the fuselage station number, which represents the axial flow line shown in Figure 3 above and is measured in inches aft from the nose of the aircraft. Station 350 corresponds to the leading edge of the wing, while 650 represents the trailing edge. As can be seen, both upwash and sidewash angles calculated with CFD correlated well with the wind tunnel data at Mach 0.8, while the results at Mach 0.95 did not match as well. The most important discrepancy is the initial peak in the sidewash angle around station number 400, shown above in Figure 7. This issue was caused by choking in the flow-through engine tube and was remedied through the use of an engine model in the flow solver. Incorporating this model significantly reduced the peak from 4.7º sidewash to just below 3º. Figure 8 below shows the new sidewash comparison.

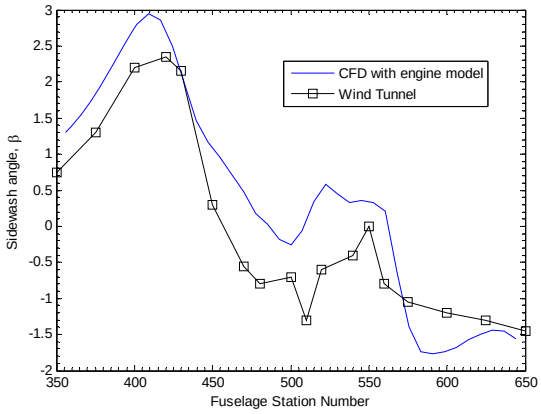

Fig 8. Sidewash angle comparison using engine model and wind tunnel at Mach 0.95

While there are still discrepancies between CFD predictions and wind tunnel results, the difference is now on the order of 0.5 degrees instead of 2.0 degrees. At this point the CFD model of the clean F-18C aircraft was considered valid and saved for further use.

2.2 Targeting Pod Flowfield Effects

The next step following validation of the aircraft model was to attach the targeting pods and examine their effect on the same axial flow line used to validate the clean F-18C. The pod geometries were obtained as computer aided design files and had not been prepared for use with CFD. The next task, therefore, was to create surface patches and background sources using these CAD files, followed by the attachment of these pods to the F-18C. These CAD files were not developed with CFD use in mind and significant time was necessary to properly manipulate these files into the correct format. A portion of each completed surface grid can be seen below in Figures 9 and 10, with the geometric differences between the two pods emphasized.

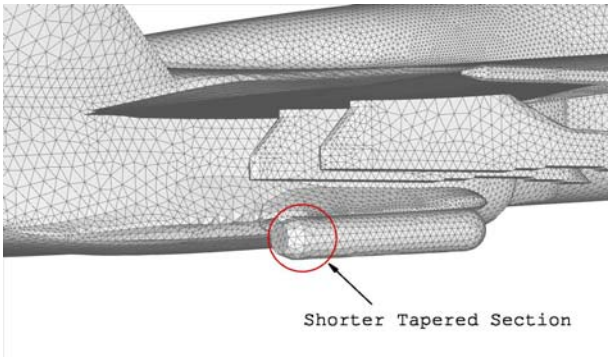

Fig 9. Surface grid of ATFLIR pod attached to F-18C aircraft

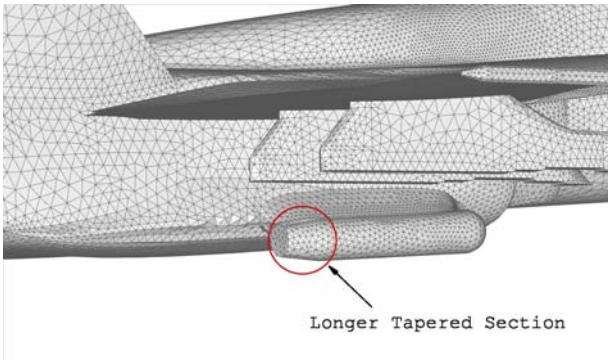

Fig 10. Surface grid of TFLIR pod attached to F-18C aircraft

Initially, it was thought that the important physical difference between the pods was the shape of the leading edge. The leading edge of the TFLIR is blunter and set farther aft, while that of the ATFLIR is more streamlined and extends farther forward. Later testing, however, revealed that the variation in aft tapering was the important distinction between the two pods. As shown, the ATFLIR has a much shorter tapered section, while the TFLIR's is longer and more gradual. Other than these minor differences, the two pods are nearly identical.

After successful grid generation, the flows around both pods were solved and data were extracted along the same axial flow line as shown in Figure 3. The results in upwash were first examined, and it was found that the addition of pods had virtually no effect on the upwash angles along the flow line. The effect of the pods on sidewash angle, however, was very significant. Figure 11 shows the details of this effect.

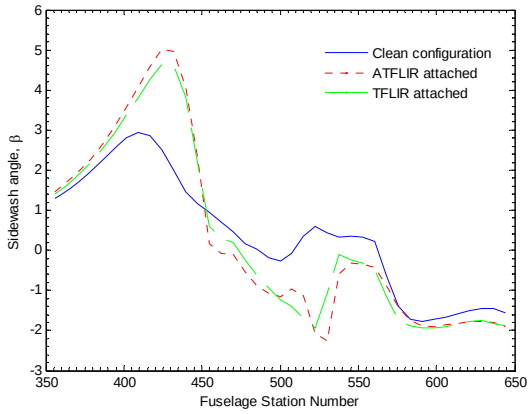

Fig 11. Effect of pods on sidewash angle along axial flow line at Mach 0.95

As this plot shows, the addition of a targeting pod dramatically increased the peak value of sidewash angle around station 425 and then decreased it near the center of the wing. It is also clear that the two pods had similar effects on the flow but were not identical. Based on slightly higher and lower peak values, this plot indicates that the ATFLIR would have a slightly greater effect on the yawing moment of a bomb beneath this pylon. While they were by no means conclusive, these results were encouraging in that they provided a qualitative indication that the pod's effects on flow sidewash angle were significant.

2.3 GBU-31 Model Validation

While the axial flow line analysis indicated that the TFLIR and ATFLIR pods had a large effect on the flow, the only way to actually demonstrate this was to introduce a store to the model and calculate the forces and moments generated on it. The store chosen for use in this analysis was the GBU-31 Joint Direct Attack Munition (JDAM).

The GBU-31 JDAM is an upgrade of the Mark 84 unguided bomb and has a standard weight of 2000 pounds, making it one of the heaviest fighter-carried weapons. The JDAM upgrade added a guidance package including an inertial navigation system, GPS receiver, movable tail control fins, and the strakes along the sides. This bomb was one of the principle stores used in the flight test program, so there are telemetry data with which to compare a

predicted trajectory. The geometry file obtained for this bomb was in CAD format and thus required extensive manipulation to prepare it for use with CFD. The completed surface grid for this bomb can be seen below in Figure 12.

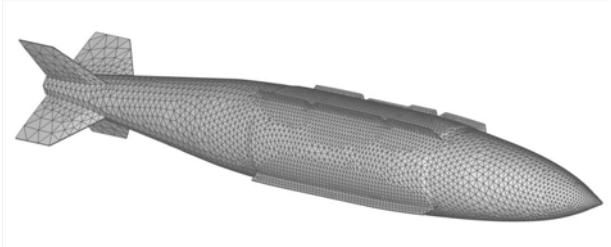

Fig 12. Surface grid of GBU-31 JDAM

Before adding the GBU-31 to the F-18C aircraft, it was necessary to validate the model of the store, again by comparison to wind tunnel results. Freestream data, in which the store is tested without an aircraft, had been previously generated in multiple large-scale wind tunnels. In these tests, the aerodynamic forces and moments generated on the store are measured with a balance.

Significant amounts of wind tunnel data have been generated at Mach 0.95, which is in the transonic region that is the focus of this project. Validation of the model was therefore undertaken at this speed using the method of an angle-of-attack sweep. In the wind tunnel, force and moment data points had been taken at numerous different angles of attack, and for the purpose of comparison, multiple angles of attack were computed using CFD as well. It is important to note that the JDAM's symmetry allowed the AOA results compared here to be directly equated to sidewash results. Figure 13 shows the normal force coefficient generated at multiple angles of attack.

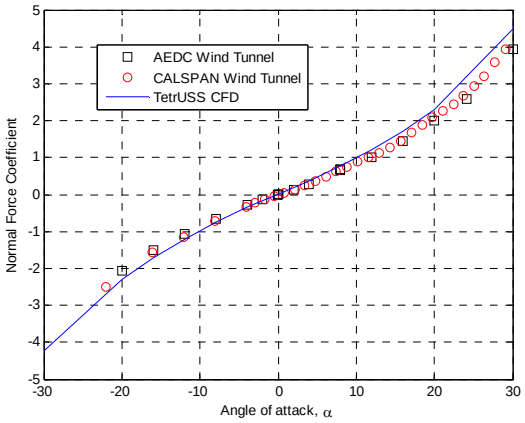

Fig 13. GBU-31 normal force coefficient at multiple angles of attack

This figure indicates good correlation between the CFD results and the measured wind tunnel data. The CFD slightly overpredicted the magnitude on both the positive and negative ends of the plot, but not enough to cause concern. Figure 14 below shows the other parameter: pitching moment coefficient. For the majority of angles of attack CFD shows good correlation, once again very slightly overpredicting the magnitudes. Around positive and negative 15º AOA, though, the wind tunnel data indicates a departure from the linear behavior that is not captured by CFD. This behavior may be caused by vortices generated on the strakes impacting the tail fins. Increased grid resolution may serve to capture this effect; alternatively, this may be caused by interference effects of the apparatus holding the store in the wind tunnel.

Figures 13 and 14 highlight the fact that wind tunnel testing and CFD analysis are not exact duplicates of each other. Each has their own strengths and weaknesses. Furthermore, even the exact geometries of the test articles in each case are slightly different than that of the actual store. Engineering approximations are made in the manufacture of the wind tunnel model as well as in the geometry definition of the CFD model.

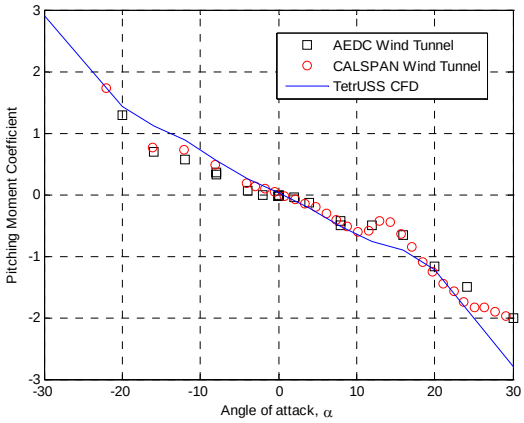

Fig 14. GBU-31 pitching moment coefficient at multiple angles of attack

Based on comparisons with large-scale wind tunnel data, this model of the GBU-31 JDAM has been considered accurate. While the variation at 15º AOA has the potential to adversely affect results it is possible that the CFD result is more accurate than the wind tunnel model; regardless, the remainder of the angle-of-attack range exhibits very close correlation.

2.4 Carriage Position Analysis

Once the models of the store and aircraft had been created and validated, the store was placed in the carriage position beneath the inboard pylon of the F-18C. Figure 15 shows the surface grid of the GBU-31 in its carriage position without a targeting pod attached to the aircraft.

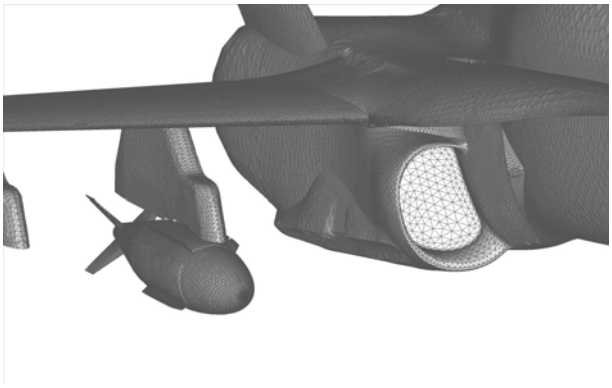

Fig 15. Surface grid of GBU-31 JDAM in carriage position with no pod

At this point in the research it was decided to add Northrop Grumman's Litening pod to this study in addition to the TFLIR and ATFLIR. The Litening pod was designed for the same purpose as the other two pods, though it incorporates some additional features and is therefore larger than the TFLIR and ATFLIR. A picture of the Litening pod attached to an F/A-18A can be seen in Figure 16.

Fig 16. Litening pod on underbelly of F/A-18A Hornet

Note that the Litening pod is larger than both other pods in length and diameter. It also features a decidedly un-aerodynamic protrusion towards its aft end that was expected to have some influence on store separation, though what the effect would be was not known.

The flight test program described in Rothback had concluded that the worst-case condition was at 0.0° aircraft AOA, so this is the condition that was tested throughout this portion of the research. This same flight test data showed that the initial trajectory of the store is very dependent upon the Mach number at which the store is released, and as a result the forces and moments on the GBU-31 were found at various Mach numbers in the transonic flight regime. Thirteen Mach numbers were chosen in the range of 0.8 to 1.05 and all four configurations, ATFLIR, TFLIR, Litening, and

clean (no pod), were examined. Resultant force and moment data were extracted for each test the two most important factors, pitching moment and yawing moment, are presented graphically in Figures 17 and 18 below. These two factors are most significant because store trajectories resulting in aircraft impact are associated with dramatic changes in the pitch and yaw angle of the store. The pitch and yaw of the store alone may be enough to swing a portion of the store (typically its tail) into the aircraft, or it may result in lateral or vertical motion that will move the store into a collision path with the aircraft.

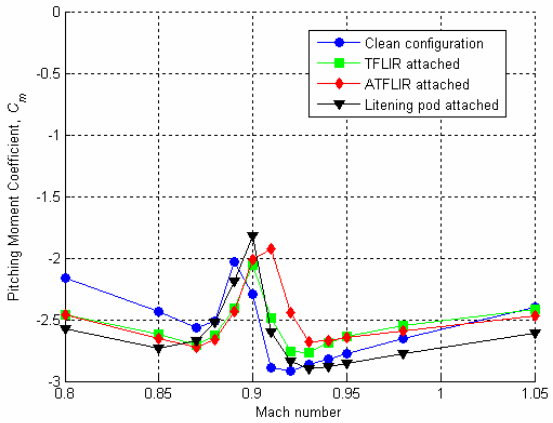

Fig 17. GBU-31 JDAM pitching moment coefficient in carriage position

As Figure 17 shows, the addition of the targeting pods does not have a very significant effect on the pitching moment of the GBU-31 in carriage position. Generally, any nose up motion of the store in the vicinity of the aircraft is dangerous. Some negative store pitching moment, which causes the nose to rotate downward, is favorable for store separation applications because the store will leave the vicinity of the aircraft more quickly. Excessive nose-down store pitching moment may not be desirable as the motion could cause the tail of the store to strike the pylon it was attached to. The store is forced away from the F-18C aircraft using fore and aft pyrotechnic ejector charges. The region in which there is variation in these data is between Mach 0.90 and 0.92. The general trend in pitching moment change with Mach number is qualitatively similar for all configurations. The region of rapid change varies slightly for each configuration with the clean configuration spiking first and the ATFLIR configuration spiking last. In all cases, the change is on the order of 1.0 from minimum negative value to maximum negative value. This change in magnitude is significant, but overshadowed by the behavior of the yawing moment which is explored next.

Figure 18 below plots yawing moment coefficient against Mach number for each of the four configurations. As can be seen, the addition of the targeting pods has a tremendous effect on this parameter.

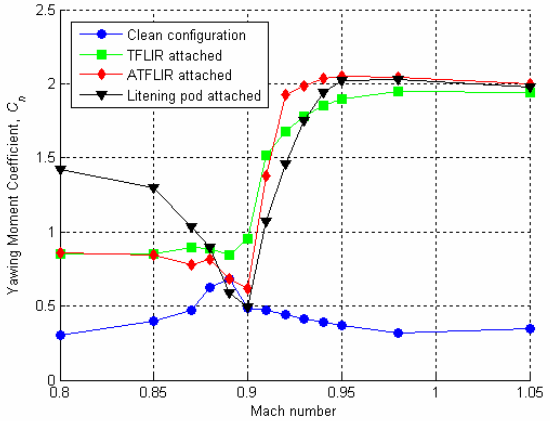

Fig 18. GBU-31 yawing moment coefficient in carriage position

In the clean configuration, the yawing moment coefficient does not vary significantly with Mach number. There is a slight peak at Mach 0.89 but this is not much greater than its value at all other Mach numbers. Clearly, the most significant aspect of this plot is the dramatic increase in yawing moment coefficient that occurs between Mach 0.90 and 0.94 in the conditions with pods attached. Over this period the coefficient rises from around 0.5 to 2.0, an increase of 300%. This increase in positive yawing moment will initially cause the bomb's nose to rotate outboard and its tail to rotate inboard. Recall that in the initial flight incident, the problem occurred when the bomb's tail fins impacted the TFLIR pod. This was the result of just such a yawing moment as predicted by these data.

2.5 Trajectory Prediction

The final steps in this store separation analysis were to predict the store's movement

following separation and to compare this prediction to flight test data. Trajectory predictions were made using the Navy Generalized Separation Package (NAVSEP), which is a software program that computes a store's position and orientation following its release.

The first task was to compare the trajectory of the store released from an aircraft in the clean configuration to a store trajectory from an aircraft with a pod attached. The ATFLIR pod was chosen for this analysis since more flight test data was available for this pod than either of the other two. Large-scale wind tunnel data were used with NAVSEP in order to calculate the trajectory of the clean configuration, while the trajectory with the ATFLIR pod was predicted using wind tunnel data augmented with CFD results. The resulting displacements in the horizontal and vertical directions are shown below in Figure 19.

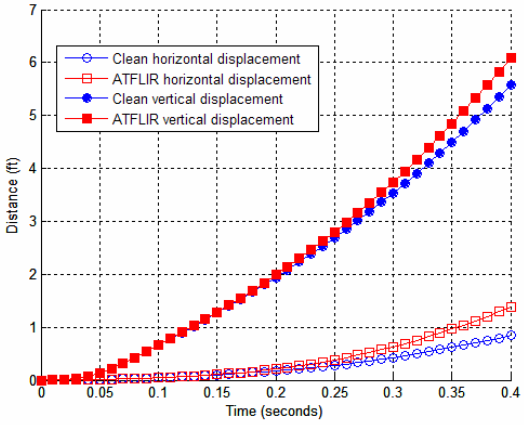

Fig 19. Predicted horizontal and vertical displacements for clean and ATFLIR cases

As this plot shows, the addition of the ATFLIR pod was predicted to cause a slight increase in the downward displacement and a 40% increase in outboard movement. In clean configuration, the store was predicted to move 0.90 feet outboard over the first 0.4 seconds after release, while with the ATFLIR attached it was expected to move 1.4 feet outboard. Moving farther outboard is not necessarily beneficial as it implies a greater yaw angle which could cause an impact of the store aft section with the ATFLIR pod. The variation in downward displacement was less than half a foot, differing between 6.1 and 5.5 feet after 0.4 seconds. This quantity is dominated by the force of the ejector so it is logical that variation would be minimal in this area.

In addition to displacements, pitch and yaw angles were also predicted for both the clean and ATFLIR cases. These results are plotted below in Figure 20.

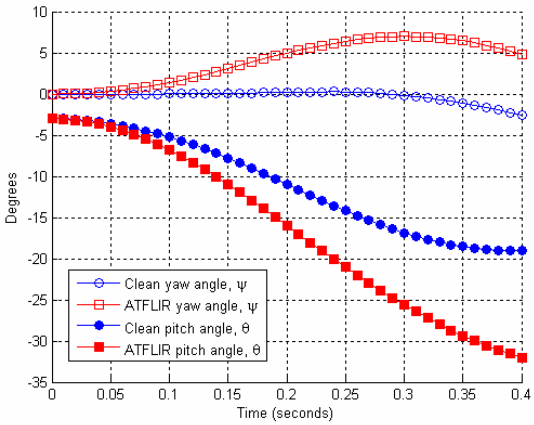

Fig 20. Predicted pitch and yaw angles for clean and ATFLIR cases

As this figure shows, the addition of the ATFLIR pod was predicted to increase both the yaw and pitch angles by a substantial amount over the clean values. The clean case was not expected to yaw at all, while the ATFLIR case was predicted to reach a yaw angle of 7.5 degrees outboard at 0.30 seconds after release. This is a substantial variation and is consistent with the pressure analysis discussed in the previous section. The pitching moment variation is also significant. The ATFLIR was predicted to cause a 68% increase over the clean value, increasing the nose-down angle from 19º to 32º 0.4 seconds after release. Such a large pitch angle can be worse than a large yawing angle, as the store can rotate so quickly that the tail moves upward and strikes the pylon. This is a particular concern with large stores such as this one, as the tail moves a greater distance upward with the same change in pitch angle.

The comparisons between the predicted clean and ATFLIR trajectories correlate with the trends that were predicted by the analysis of forces and moments on the store in the carriage position. In order to validate these data it was necessary to compare the predicted trajectories with actual flight test results. Therefore trajectories were compared for both the clean

and ATFLIR cases using vertical position, horizontal position, yaw angle, and pitch angle. The plots for vertical and horizontal position can be seen below in Figures 21 and 22.

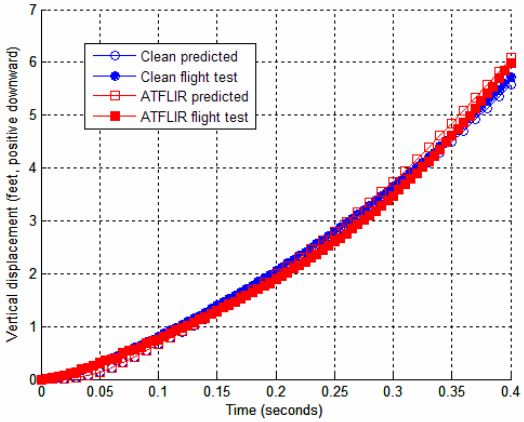

Fig 21. Vertical position flight test comparison

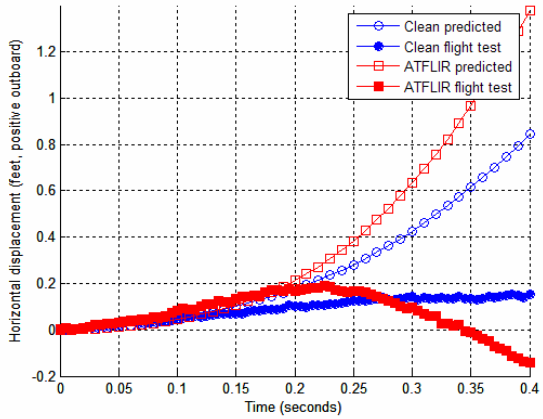

Fig 22. Horizontal position flight test comparison

As the first plot shows, the predicted vertical position results match almost perfectly with flight test data, indicating a good model of the ejector system. Results in horizontal displacement diverged at the later time portion but did match well for the first 0.2 seconds. The variation is much greater between the predicted and actual ATFLIR results than it is between the predicted and actual clean results. This difference is likely due to the manner in which the CFD data was used to augment the wind tunnel data, which provided the most accuracy near the carriage position and became less accurate as the store moved farther away. This would explain why the results match well initially and diverged at later times. Another possible explanation for the difference in spatial displacements is associated with the manner in which the data is captured from flight test. In this case, the flight test data came from photogrammetrics. The camera images used as the basis for photogrammetric calculations are obtained from cameras primarily situated abeam the delivery aircraft. Depth in the frame of the camera is associated with y-displacement and has a higher degree of uncertainty than do the vertical and axial displacements. The magnitude and direction of the movement in the horizontal direction are so small, though, that this variation is not overly critical. The worst case flight result showed the ATFLIR moving less than 3.0 inches towards the aircraft after 0.4 seconds, by which time the store has already moved 6.0 feet downward.

The other two plots generated in this section compare the yaw and pitch angles between the predicted and flight test cases. These plots can be seen below in Figures 23 and 24.

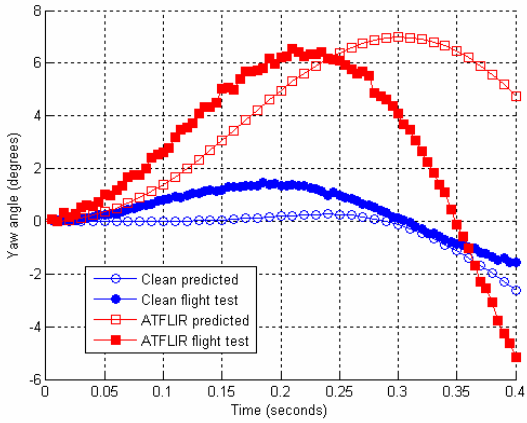

Fig 23. Yaw angle flight test comparison

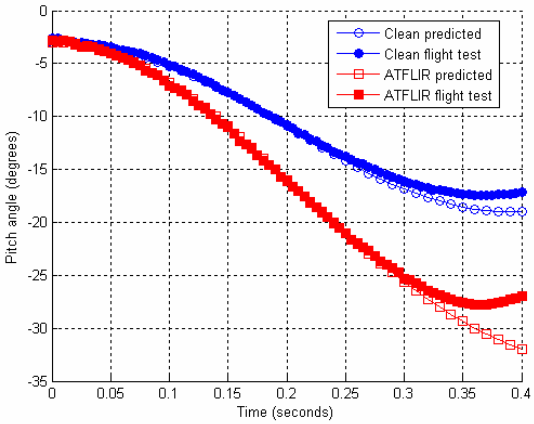

Fig 24. Pitch angle flight test comparison

Both of these plots reveal good correlation between the predicted trajectory and flight test results. The predicted maximum yaw angle is a mere 0.3° from the actual one, with the predicted value showing the slightly higher value of 7.0°. The correlation of the predicted clean trajectory was good as well, never varying by more than two degrees. The greatest discrepancy on this plot is the variation of the ATFLIR results at later times. This difference is possibly due to errors in the method used to calculate the flight test results. Even so, it is noteworthy that the prediction exhibited the same trends and maximum as the flight test result. At lower times it is also important that the prediction was a few degrees lower in both the clean and ATFLIR cases, which shows that that prediction accurately captured the differences between the cases in carriage position. The comparison of pitch angle in Fig 24 is an even better match than yaw angle. As this plot shows, the predicted values were exact matches for flight test results for the first 0.3 seconds after release. Such a change in pitch angle can cause significant problems for stores so it is important that this result was accurately captured.

Based on these comparisons of predicted and actual trajectories for both the clean and ATFLIR configurations, as well as previous validations of both the F-18C aircraft and GBU-31 JDAM, the data generated in this project were considered accurate and accepted for further use.

3 Analysis

While the results presented up to this point have demonstrated the applicability of CFD to store separation analysis, no effort has been made to explain the actual phenomenon causing the targeting pods to influence the forces and moments on the store. This is one area in which CFD can provide insight into aspects of the flowfield that cannot be obtained from either typical store separation wind tunnel data or flight testing. CFD is the only method which can provide detailed surface pressure distributions as well as flow properties at all points. There are developing capabilities to enable surface pressure calculation in the wind tunnel, but these are not yet widely available.

The large quantities of data generated in CFD studies requires specialized flow visualization programs to analyze such large amounts of raw data, and in this research project Amtec Engineering's Tecplot® was used for this purpose. Tecplot® is an advanced graphics program designed for many types of engineering data. Important features pertinent to this project include the ability to display pressure surface pressure contours and calculate the location of shocks in the flow. The method in which Tecplot® calculates shock locations can be seen in ref [3].

3.1 Shock Analysis

All store separation issues involving these pods occurred in the transonic flight regime, making the formation of shocks a likely aspect of the problem. Unfortunately, while shocks can be calculated analytically over basic configurations they are very difficult to predict over complex geometries such as the one analyzed here, making CFD an ideal tool for this investigation.

Figures 25-27 below show the location of shocks on the underside of the F-18C with ATFLIR pod and the GBU-31 JDAM in the carriage position. These figures show the same region at Mach 0.85, 0.90, and 0.95 respectively, and were mirrored to show the shock locations on the left side and surface pressures on the right. An examination of these figures show that there are two distinct shocks forming on the ATFLIR pod, one near the nose of the pod and one at its trailing edge. Both of these shocks impact the GBU-31 JDAM in its carriage position. The leading shock impacts the bomb near its center, while the trailing shock impacts near the fins. Recall that initial speculation centered on the difference in leading edge geometry between the ATFLIR and TFLIR as the likely explanation for their different effects on store trajectory. As a result of this hypothesis, the leading edge shock was examined first. While this leading edge shock did cause a change in pressure where it impacted the store, it was soon found to remain

relatively consistent with changing Mach number. A visual examination of this shock at various Mach numbers showed that it did not move or change the surface pressures enough to cause the drastic change in store yawing moment as predicted by CFD results.

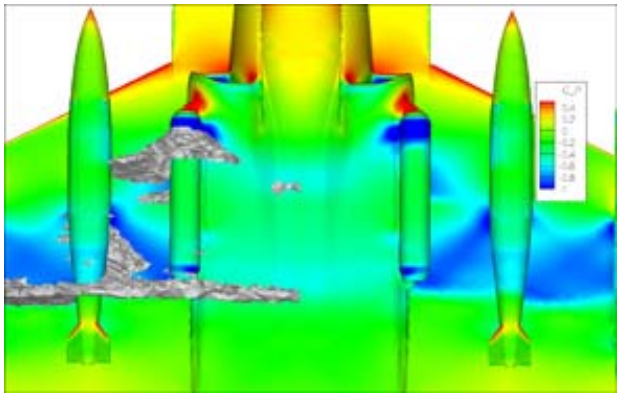

Fig 25. Shock formation on F-18C underbelly with ATFLIR pod at Mach 0.85

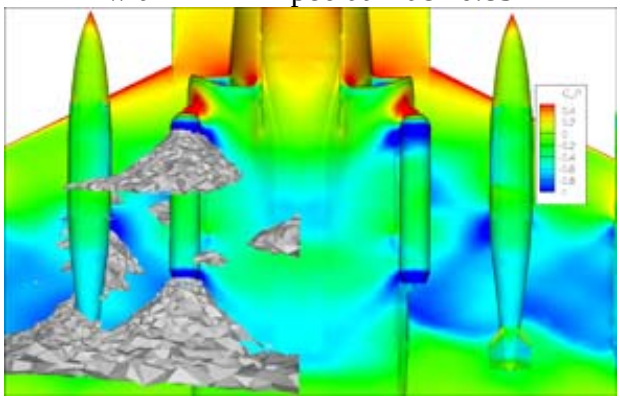

Fig 26. Shock formation on F-18C underbelly with ATFLIR pod at Mach 0.90

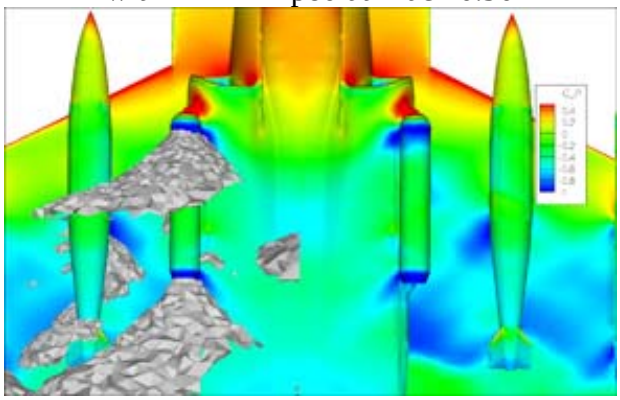

Fig 27. Shock formation on F-18C underbelly with ATFLIR pod at Mach 0.95

As these images show, the shock produced by the trailing edge of the ATFLIR pod does move a significant amount over this range of Mach numbers. The shock is barely formed at Mach 0.85, impacts the tail at 0.90, and aft of the tail by 0.95. By contrast, the shock produced by the leading edge impacts the GBU-31 JDAM at the same location regardless of speed. While these images do not give any quantitative data, they strongly suggest that the trailing shock is the cause of the pressure changes.

In order to ensure that these shocks only formed due to the presence of the ATFLIR pod, images from the same perspective and at the same flight conditions were made for the case with no targeting pod. These can be seen below in Figures 28-30.

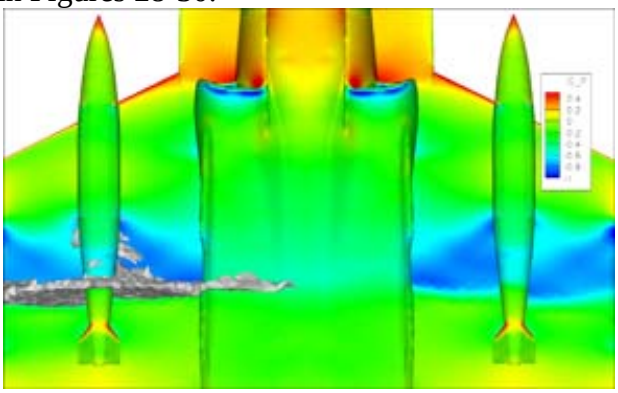

Fig 28. Shock formation on F-18C underbelly at Mach 0.85 in clean configuration

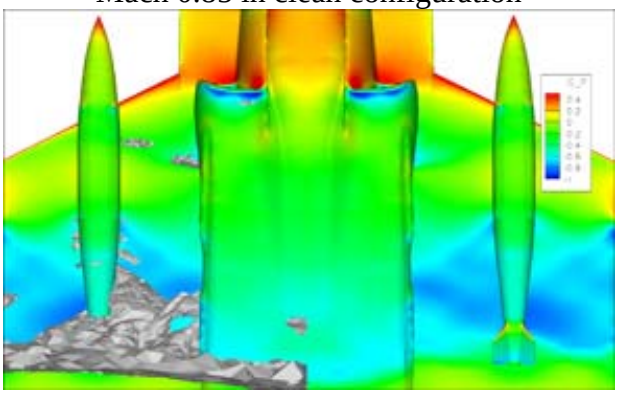

Fig 29. Shock formation on F-18C underbelly at Mach 0.90 in clean configuration

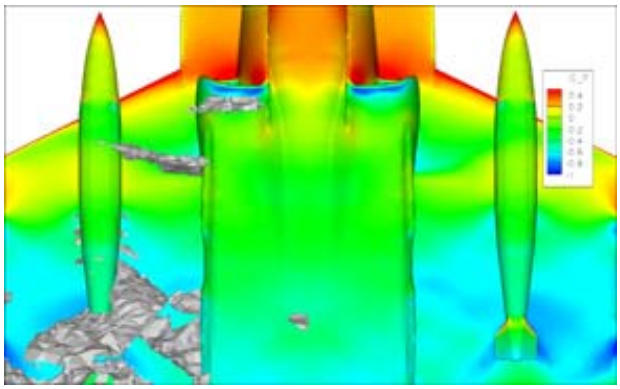

Fig 30. Shock formation on F-18C underbelly at Mach 0.95 in clean configuration

As these plots show, there is a shock that moves aft in the clean configuration. This shock, however, is nearly symmetric and does not cause as intense a change in surface pressures as the shock from the ATFLIR does. In the case of the ATFLIR, there is a distinct line on the underside of the wing where low pressure became high pressure. This transition is much more gradual at higher speeds in the clean configuration.

3.2 Component Analysis

Based on the observations made when analyzing shock formation, it was likely that a shock impacting the tail caused the variation in store yawing moment. In order to prove whether or not this was the case, the GBU-31 JDAM was divided into three regions and each was analyzed separately. The regions analyzed were the forebody, midsection, and tail, as shown in Figure 31.

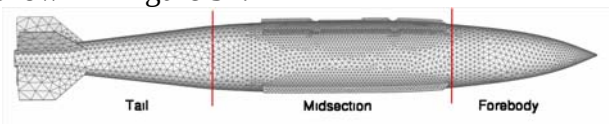

Fig 31. JDAM component locations

Version 6.0 of the flow solver USM3D allowed for the integration of pressures on multiple components, so this feature was used to determine the contribution made by each component to the store's total forces and moments. Figures 32 and 33 show the contributions to yawing moment made by the forebody and midsection, respectively. While both sections of the store show a higher yawing moment produced by the cases with pods attached, the magnitude of the differences is quite low. The largest change on the forebody is a difference of 0.20 between the Litening pod and the clean configuration. This variation is also constant across all Mach numbers, so the forebody has no net effect on the total yawing moment spike at Mach 0.90.

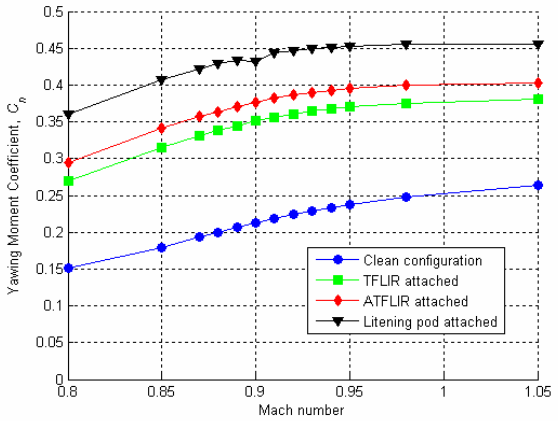

Fig 32. GBU-31 JDAM forebody yawing moment component

The midsection of the GBU-31 JDAM was shown to be nearly as insignificant as the forebody in terms of yawing moment. Figure 33 below shows the variation in this quantity, and as similar to the forebody the greatest variation was only 0.30. This result proved that the shock formed on the leading edge of the ATFLIR pod did not have an effect on the yawing moment variation. This conclusion was drawn from an examination of shock positioning and reinforced numerically with these results.

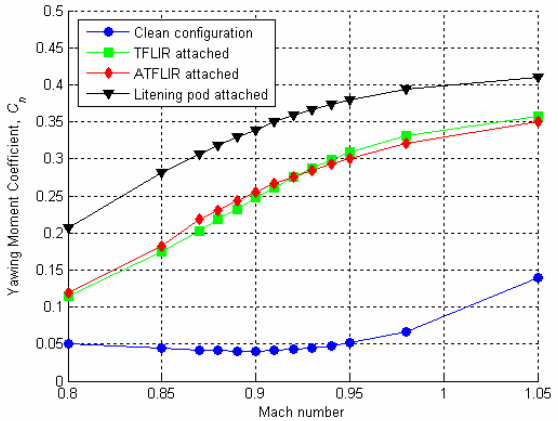

Fig 33. GBU-31 JDAM midsection yawing moment component

If both the forebody and midsection of the GBU-31 JDAM showed minimal change in yawing moment as Mach number increased, the tail had to be the important feature in this regard. Figure 34 below shows that this was the case. In clean configuration, the yawing moment caused by the tail remained relatively constant, varying by only 0.40. This configuration peaked at Mach 0.89, which is near the speed where the pod configurations minimized.

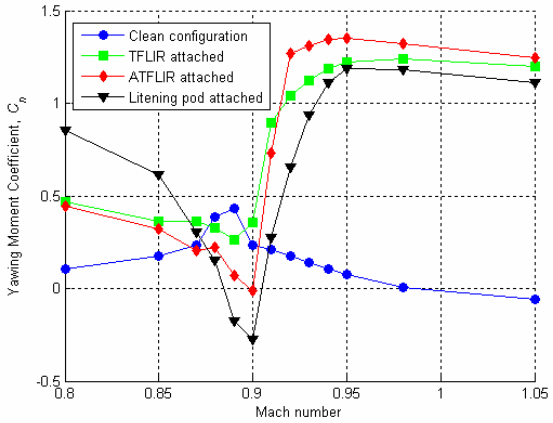

Fig 34. GBU-31 JDAM tail yawing moment component

As this plot reveals, the tail was clearly the most critical portion of the store. It exhibited dramatic changes in yawing moment, most especially from Mach 0.90 to 0.92. Recall from the images in Figures 25-27 that this is the same speed range when the trailing edge shock was sweeping across the tail. At this point it could be concluded that the trailing edge shock was the cause of the shift in yawing moment, but just to be sure images of the pressure distributions on the inboard and outboard sides of the bomb's tail were generated at Mach numbers in this region. The range of Mach 0.90 to 0.92 can be seen in Figures 35-37 below.

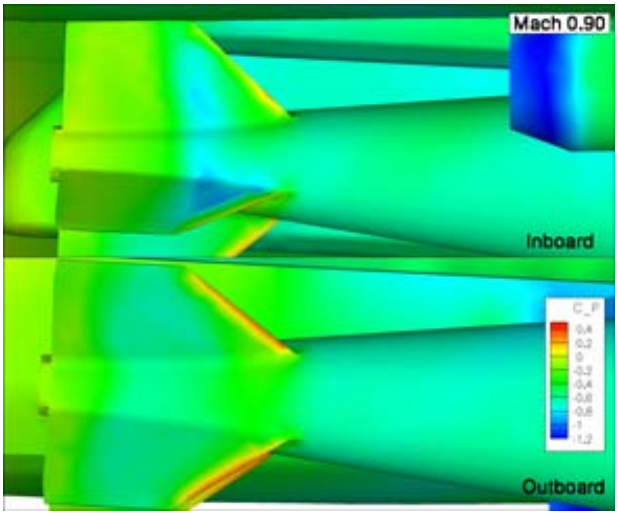

Fig 35. GBU-31 JDAM tail pressure distribution at Mach 0.90

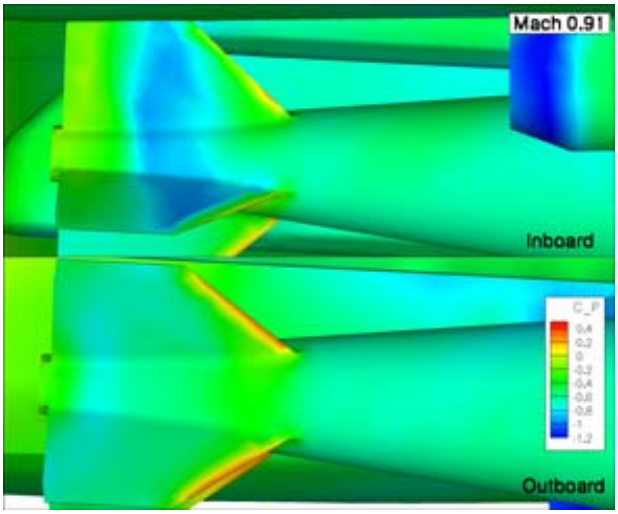

Fig 36. GBU-31 JDAM tail pressure distribution at Mach 0.91

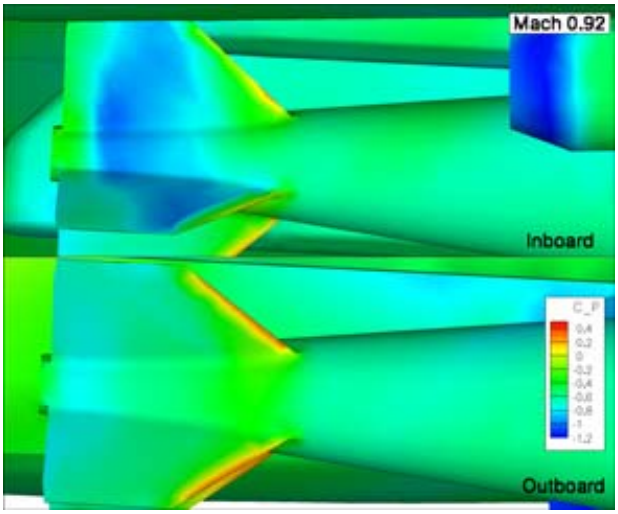

Fig 37. GBU-31 JDAM tail pressure distribution at Mach 0.92

As these figures show, the pressure on the outboard side of the tail remains relatively constant while the inboard side changes quite a bit. At Mach 0.90 the majority of the inboard section of the tail is at a relatively high pressure (in green and yellow), representing a pressure coefficient value of around 0.0. There is only a small region of low pressure (in blue) on the front portion of the fins, which represents a much lower pressure coefficient of -1.0. A variation of 1.0 in pressure coefficient is a very significant difference, indicating that the region of lower static pressure is experiencing nearly double the dynamic pressure of the region in greenish-yellow. The division between the high and low pressure regions moves aft as speed increases, which significantly decreases the overall static pressure on the inboard side of the store. The pressure on the outboard side of the tail remains relatively constant through this speed range, so the decrease in pressure on the inboard side causes a pressure imbalance which results in a net aerodynamic force pushing the tail inboard. This force is therefore the cause of the store yawing moment change shown to occur over this range of velocities. The cause of the division between areas of low and high pressure on the tail's inboard side is the impact of the shock generated on the trailing edge of the ATFLIR pod. As stated previously, an important property of shocks is that they cause an increase in static pressure when they occur. A shock is in fact the only explanation for such a dramatic increase in pressure along flat surfaces such as these tail fins. The sweeping of the ATFLIR's trailing shock is the reason that the area of lower pressure on the tail continued to grow until the entire inboard side was at the lower pressure. These images are final confirmation that the trailing edge shock from the ATFLIR was the cause of the store's drastic increase in yawing moment.

4 Conclusions

The solution of complex flow problems using computational fluid dynamics is increasingly being used to augment traditional methods of aerodynamic testing, such as the use of wind tunnel and flight tests. This is especially true in the field of store separation, where the past two decades have seen CFD make significant contributions to the field in many areas. CFD has been particularly useful in store separation applications that simply cannot be replicated in the wind tunnel or can only be replicated with great difficulty. An example of this includes such applications as the release of a store from a cavity such as a bomb bay of a B-1B aircraft. CFD has also proved to be useful in the visualization of complex flows in order to better understand the elements that affect such flows. This research has demonstrated the use of CFD as a flow visualization tool to capture a complex shock interaction between a store and an element of the F-18C aircraft geometry, namely the targeting pod. In addition to identification of the changes in aircraft geometry resulting in adverse store separation conditions, CFD was also able to quantify those adverse effects. The quantified effects then served as input to a trajectory simulation program which used the best available data from ejector force data, wind tunnel testing, and CFD to predict the motion of the store after release. The predicted motion of the store and quantified effects of the transonic flow on the store correlated well with the observed behavior of the shock interference in the flow. This led to a number of recommendations concerning the trailing-edge geometry of the targeting pod on the F-18C that could potentially result in significant increases in combat effectiveness.

CFD is, however, not an experimental method but an approximate solution to a set of equations which have no known analytic solution. As such, the process of validation of each step of a CFD investigation is as important as the results themselves. CFD results without proper verification and validation lack the pedigree to provide the store separation engineer with the confidence to make flight clearance decisions. Therefore each step in the analysis of the store separation simulation using CFD was verified against existing wind tunnel and flight test data. Excellent agreement was found for the freestream flow characteristics of the GBU-XX store using CFD to large scale wind tunnel testing in two separate wind tunnels. Flow quality of the CFD solution

around the F-18C aircraft itself was verified at the carriage location of the store against existing wind tunnel data, and engine parameters in the CFD model were tuned appropriately. Finally, the predicted trajectory of the store after release using results from CFD was validated against flight test data for the release of the store from a similar condition. Good agreement was found in each case, giving the store separation engineer the confidence in both the predicted trajectory of the store and the rationale for the adverse deviation of the predicted trajectory from nominal when a targeting pod is attached to the aircraft.

This research effort has proven the efficacy of computational fluid dynamics to the field of store separation analysis. CFD methods were used to accurately model complex aircraft geometries and generate results consistent with those produced by the wind tunnel and flight testing. The analysis of subtle geometric changes was quantified, which enabled the determination of the specific aspect of the geometry which caused the detrimental effect. A more thorough, accurate, and insightful understanding of the store separation environment of the F-18C carrying a targeting pod in the transonic flow regime was obtained.

4.1 Future Work

Future research will focus on the effect of geometric modifications to the trailing end of the targeting pods. It is expected that a smoother trailing end will weaken shock formation and thus mitigate the adverse conditions currently experienced. Additional research could also refine the trajectory predictions using CFD data in lieu of wind tunnel data employed in this effort.

References

[1] Rothback, N., and Cenko, A., “Dangers of Aircraft Modifications Without Conducting an Investigation into the Effects on the Aircraft Flowfield and Flying Qualities,” 2001, p. 1.

[2] Rothback, N., and Cenko, A., “Dangers of Aircraft Modifications Without Conducting an Investigation into the Effects on the Aircraft Flowfield and Flying Qualities,” 2001, p. 1.

[3] Lovely, D., and Haimes, R., “Shock Detection from Compuational Fluid Dynamics Results,” AIAA Paper 99-3285, 1999.

Copyright Statement